Synthesis and Characterization of Blue Faceted Anatase Nanoparticles through Extensive Fluorine Lattice Doping

David G. Calatayud,[*,†,▽] Teresa Jardiel,[†] Marco Peiteado,[‡] Francesc Illas,[§] Elio Giamello,[⊥] Francisco J. Palomares,[∥] Daniel Fernández-Hevia,[#,○] and Amador C. Caballero[†]

[†]Department of Electroceramics, Instituto de Cerámica y Vidrio (CSIC), Kelsen 5, 28049, Madrid, Spain

[‡]POEMMA-CEMDATIC, ETSI Telecomunicación (UPM), Avenue Complutense 30, 28040 Madrid, Spain

[§]Departament de Química Física & IQTCUB, Universitat de Barcelona, C/Martí i Franquès 1, 08028, Barcelona, Spain

[⊥]Dipartimento di Chimica and NIS, Università di Torino, Via P. Giuria 7, 10125 Torino, Italy

[∥]Department of Nanostructures and Surfaces, Instituto de Ciencia de Materiales de Madrid, CSIC, c/Sor Juana Inés de la Cruz 3, Campus de Cantoblanco, 28049 Madrid, Spain

[#]Department of Chemistry, Group of Photocatalysis and Spectroscopy Applied to the Environment (FEAM), Universidad de Las Palmas de Gran Canaria, Campus de Tafira, Gran Canaria 35017, Spain

[○]INAEL Electrical Systems, S.A. c/Jarama 5, Toledo 45007, Spain

ABSTRACT: An effective synthesis strategy for the extensive fluorination of the TiO_2 anatase lattice has been developed which provides a highly stable blue-colored titania powder. The process also produces a convenient faceted morphology of the doped nanoparticles. Both theoretical and experimental data indicate an ordered atomic structure, in which an exceptionally high amount of fluorine ions substitute oxygen ions in the TiO_2 lattice. The extra-electrons borne by fluorine are stabilized by lattice Ti cations via a mechanism of valence induction, eventually leading to a consequent high amount of reduced Ti^{3+} centers. Such structure, whose general formula can be expressed as $Ti^{4+}_{(1-x)}Ti^{3+}_{x}O^{2-}_{(2-x)}F^{-}_{x}$, confers an excellent stability to the as-synthesized nanoparticles (in spite of the excess electrons), explaining for example why the blue color is retained even upon storage in ambient atmosphere. But moreover, the high concentration of the relatively shallow Ti^{3+} generated states also form a sort of sub-band close to the bottom of the conduction band itself. The whole effect results in a tangible decrease (0.2 eV) of the anatase band gap which allows an inspiring upgrading of its UV photocatalytic activity. Our results also suggest that narrowing the band gap is insufficient for a substantial improvement in the visible light harvesting.

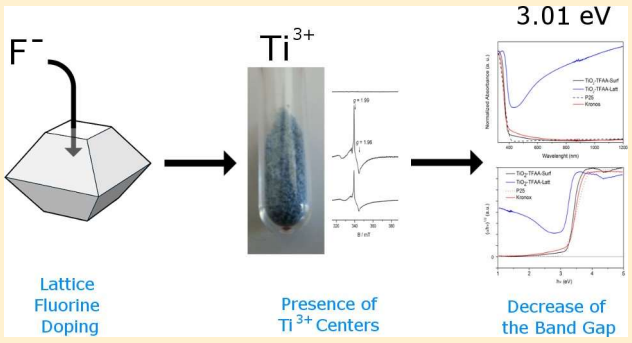

1. INTRODUCTION

Current research endeavors in the field of semiconductor photocatalysts are widely focused on the sustainable production of TiO_2 anatase nanomaterials for environmental purification, hydrogen generation and/or solar energy conversion.[1−7] Among the key parameters boosting the photocatalytic efficiency of anatase nanoparticles, an increased light absorption to extend the optical response to the visible or even the near-infrared region, together with an improved charge separation of the electrons and holes generated upon photoexcitation, shall be enumerated.[8−10] Additionally, given that a variety of physical and chemical processes take place on the surface (viz. adsorption of reactant molecules, surface transfer of photo-excited electrons to reactant molecules, and desorption of product molecules), an enhanced surface reactivity of the TiO_2 particles will be also paramount for the photocatalytic performance of these materials.[11,12] A careful look to the specialized literature reveals that the problems with the surface reactivity are in the process of being solved. Working on the processing strategy, a collective exposition of the three fundamental low-index facets of TiO_2 anatase crystals can be more or less ensured to yield a more efficient photocatalytic response.[7,13−19] So far, the best scenario has been found when employing fluorine-based compounds as dopants, since fluorine atoms can act as both morphology directors and electron scavengers to reduce the recombination rate of electrons and holes.[20−26] However, the F-doped anatase materials produced so far still fail to meet some crucial engineering requirements, exhibiting a too poor behavior in the visible region. Several factors may account for this inconvenience, but undoubtedly the electronic structure of TiO_2 anatase is decisive. TiO_2 anatase has a bandgap of 3.2 eV which only allows the

DOI: 10.1021/acs.jpcc.5b06923

excitation of carriers by light with wavelengths smaller than 387 nm;[1] if visible light harvesting is to be enabled, this gap should be narrowed. Chemical doping is known as an effective method to narrow the bandgap, and fluorine, in particular, has been proposed as a feasible candidate to modulate that of TiO_2,[27,28] although the consequences for photocatalysis remain unclear. Up to date, however, most attempts to reduce the band gap of anatase through fluorine doping has resulted little operative. Now there is evidence that this debacle could be attributed to the doping process itself, or to be more precise, to the magnitude of the doping process: the synthetic processes employed to prepare F-doped anatase more or less succeed in attaining a functional surface doping of the TiO_2 nanoparticles, but an effective F-doping of the TiO_2 lattice is more difficult to guarantee. For example, in a previous work, we developed a one-step semi solvothermal methodology in which by using trifluoroacetic acid (TFAA) as both capping agent and electron scavenger, highly crystalline anatase nanoparticles with an upgraded photocatalytic response were successfully prepared.[29] As we attested, fluorine primarily adsorbs on the surface of the TiO_2 nanoparticles either through the oxygen atoms of the TFAA molecule itself or as fluorine ions released from the partial decomposition of TFAA. That is to say, the incorporated fluorine species firmly modify the surface of the anatase nanoparticles and improve their photoreactivity, but actually a bulk homogeneous doping of the crystal lattice is not really accomplished. As a straight consequence the band gap of the produced nanoparticles barely changes from that of pure TiO_2. Feasibly, an effective F-doping of the TiO_2 lattice will produce a different score, but then the following question must be responded: is it really possible to achieve such uniform lattice doping?

Theoretical Premise. To answer this question we have executed some periodic density functional calculations, mostly aimed to figure out if fluorine atoms can indeed enter the anatase structure and how they do it. In a first series of calculations,[30] the thermodynamic stability of F-doped anatase was investigated using large enough supercells; these are needed to guarantee that the dopant concentration in the computational models (~1%) is close (or not too far) from the values in the experimental samples. The results revealed that substitutional (O by F) F doping of bulk anatase, but also of rutile and brookite, is always thermodynamically favored. In order to investigate how F can reach appropriate sites of bulk TiO_2 anatase, F diffusion through the material was also considered using a similar approach.[31] Results consistently showed that, in the case of anatase, the strong relaxation of the substrate in response to the presence of the dopant leads to relatively small energy barriers for diffusion which, in the case of the [100] direction appears to almost vanish. Consequently, F-doping is thermodynamically favored and the presence of F in the vicinity of O sites in the bulk of anatase becomes possible thanks to the low energy barriers for diffusion. Obviously, diffusion can only start once the corresponding surfaces are fully covered with F. Again, the density functional calculations show that F adsorption is exothermic and that the presence of F has a differential effect on the different surfaces, stabilizing the more reactive (001) surface and destabilizing the more stable (in absence of F) (101) surface.[32] To summarize, the periodic density functional calculations strongly suggest that F doping is possible and the mechanism involves surface covering and diffusion through the bulk. In this way, F at the surface and at interstitial sites during diffusion provides a reservoir for O substitution by F which can be used in other processes.

Now looking back to our synthesis methodology, we have identified one key feature which may explain the difficulties to effectively dope the anatase lattice: as witnessed by X-ray photoelectron spectroscopy (XPS) and Fourier transform infrared spectroscopy (FTIR) measurements[29] a considerable number of TFFA molecules remains unabridged after the solvothermal process and, consequently, the amount of free fluorine ions to enter the TiO_2 lattice is eventually too low. Our previous experience with this system suggests that increasing the amount of TFFA added to the starting pot essentially leads to unwelcome morphologies, poorly faceted anatase nanoparticles and/or broadened size distributions. Conversely, when introducing subtle changes in the experimental conditions, the degradation of the TFAA molecule can be encouraged without altering the targeted crystal growth habit. In particular the greatest scores have come when shifting the temperature of the solvothermal process. As indicated, the introduced change had to be fairly smooth: the maximum temperature was slightly increased from 200 to 235 °C, but as results will here demonstrate this is fairly enough to largely degrade the TFFA, to increase the amount of released fluorine ions that could enter the TiO_2 lattice and, eventually, to successfully change the photocatalytic activity of the resulting TiO_2 nanoparticles, presumably through bandgap narrowing.

2. EXPERIMENTAL SECTION

Synthesis of TFAA-Modified Anatase TiO_2 Nanoparticles. Well-faceted nanoparticles of TiO_2 have been synthesized through a one-step semisolvothermal route using as received titanium(IV) tetrabutoxide ($Ti(OBut)_4$, Fluka, 98%) and trifluoroacetic acid (CF_3COOH, Aldrich, 70%, TFAA). Compared with other alkyl precursors, the butoxide group of $Ti(OBut)_4$ exhibits a slower rate of hydrolysis, thereby allowing an enhanced control of the diffusion and polymerization processes.[29] In a typical procedure 5 mL of $Ti(OBut)_4$ are introduced in a 50 mL Teflon-lined stainless steel autoclave, together with 1.9 g of TFAA. A small amount of deionized water (0.4 mL) is added to accelerate the hydrolysis reaction. The system is then heated at 235 °C for 24 h. The obtained precipitate is washed several times with water and ethanol (96%) and finally dried at 105 °C.

Hereafter this powder will be quoted as TiO_2-TFAA-Latt (i.e., lattice-doped nanoparticles), as distinctive from our previous surface-doped powder, TiO_2-TFFA-Surf.

Processing and Characterization Methods. A comprehensive examination of the obtained powders was conducted using a broad set of characterization techniques. The analyses of the crystalline structure and the phase identification were performed by X-ray diffraction (XRD Bruker D8 ADVANCE, Madison, WI) with a monochromatized source of Cu $K\alpha_1$ radiation (λ = 1.5406 nm) at 1.6 kW (40 kV, 40 mA); samples were prepared by placing a drop of a concentrated ethanol dispersion of particles onto a single crystal silicon plate. Transmission electron microscopy (TEM) images were obtained on a JEOL 2100 F TEM/STEM (Tokyo, Japan) operating at 200 kV and equipped with a field emission electron gun providing a point resolution of 0.19 nm; samples were prepared by placing a drop of a dilute ethanol dispersion of nanoparticles onto a 300-mesh carbon-coated copper grid and evaporated immediately at 60 °C.

DOI: 10.1021/acs.jpcc.5b06923

X-ray photoelectron spectroscopy (XPS) was used to characterize the chemical composition of the samples. XPS spectra were acquired in an ultrahigh vacuum (UHV) chamber with a base pressure of 1×10^{-9} mbar using a hemispherical electron energy analyzer (SPECS Phoibos 150 spectrometer) and a monochromatic Al Kα X-ray source (1486.74 eV). XPS spectra were recorded at the normal emission takeoff angle, using an energy step of 0.05 eV and a pass-energy of 10 eV for high resolution data, which provides an overall instrumental peak broadening of 0.4 eV.[33] Carbon and hydroxyl (OH) species were also detected as surface contaminants and the signal from adventitious carbon at 284.6 eV was used for energy calibration. Data processing was performed using CasaXPS software.

The infrared spectra of the samples were obtained on Fourier transform infrared spectrometer Thermo Nicolet 6700 FTIR equipment by using the attenuated total reflectance (ATR) method (polyethylene detector). The obtained spectra were averaged from a minimum of 512 scans.

Electron paramagnetic resonance (EPR) spectra, recorded either at room temperature or at liquid nitrogen temperature (77K), were run on a X-band CW-EPR Bruker EMX spectrometer equipped with a cylindrical cavity operating at 100 kHz field modulation.

UV−vis−NIR diffuse reflectance spectroscopy (DRS UV−vis−NIR) was carried out on a PerkinElmer Lambda 950 UV/vis spectrometer (Waltham, MA) equipped with an integrating sphere.

Testing of Photocatalytic Activity. The photocatalytic performance of the powders prepared in this study was evaluated in the following way: 50 mg of powder were initially suspended in an aqueous solution of methyl orange (10^{-5} M, 100 mL) using a quartz reactor. The suspension, kept under magnetic stirring, was then irradiated using a high-pressure mercury vapor lamp (250 W, HPL-N Philips, Amsterdam, The Netherlands) for UV irradiation and a tungsten lamp (500 W, General Electrics, USA) with a filter to remove the UV component for visible irradiation. Four ml aliquots were taken progressively from the suspension after different irradiation times. The supernatant and the solid particles were separated by centrifugation at 6,000 rpm. The absorption spectrum of the supernatant solution was measured on a PerkinElmer Lambda 950 UV/vis spectrometer (Waltham, MA), and the concentration (degradation) of methyl orange was determined monitoring the changes in the absorbance at 465 nm. On collecting these data, two side effects must be considered which may lead to a misinterpreted decreased value in the methyl orange concentration: the self-degradation of the methyl orange molecule under the irradiation, as well as its incidental (partial) absorption to the surface of the TiO_2 particles. In this contribution, both scenarios were contemplated as follows: on the one hand, a blank solution of methyl orange with no TiO_2 powder was irradiated under the same experimental conditions; as it was observed, in the absence of our anatase particles, no degradation of methyl orange was indeed produced. On the other hand, suspensions with methyl orange and the different TiO_2 powders were prepared as described before but they were not subjected to irradiation: in such dark conditions, no changes in the methyl orange concentration were observed for these suspensions all along the test, so absorption to the TiO_2 surface was discarded in all cases.

3. RESULTS

The first evidence of a different scenario after modifying the synthesis conditions was found in the color of the obtained powder. In the preceding experiment conducted at 200 °C, the dried precipitate was initially brown colored and it had to be cleaned under UV−vis irradiation to remove the unreacted organic matter; a white powder was then obtained (TiO_2-TFAA-Surf).[29] Now, the increase in the reaction temperature produces a blue powder after drying the precipitate, with no need for further cleaning (Figure 1a). This bluish tone has been

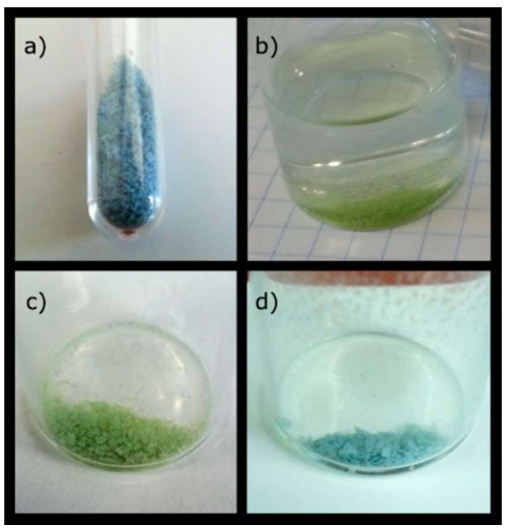

Figure 1. Different pictures of the TiO_2-TFAA-Latt powder: (a) as-synthesized, (b) submerged in H_2O_2, (c) right after removing the H_2O_2, and (d) several days after the H_2O_2 treatment.

already related to the occurrence of Ti^{3+} centers in reduced TiO_2;[34−37] in some of these previous experiments, however, the blue color irrevocably disappears after further annealing or after a long air exposure, indicating a reversible $Ti^{4+} \leftrightarrow Ti^{3+}$ redox process.[37] In the present sample no such loss of the blue color is observed; moreover, although an aggressive treatment with H_2O_2 to oxidize the surface initially turns the precipitate to yellow shade (Figures 1, parts b and c), several days after removing the peroxide the blue color is completely spontaneously recovered (Figure 1d).

The crystal structure of the blue powder was investigated by X-ray diffraction (Figure 2). As happened with the sample synthesized at 200 °C, a crystalline single-phase pattern

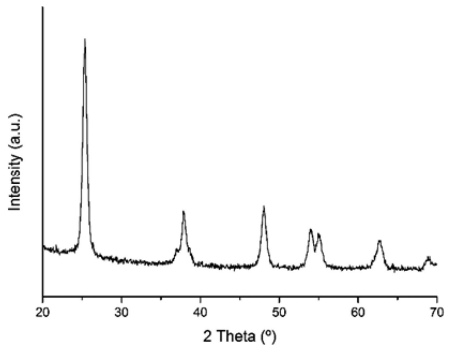

Figure 2. X-ray diffraction pattern for the synthesized TiO_2-TFAA-Latt powder. All peaks corresponding to the anatase TiO_2 phase.

DOI: 10.1021/acs.jpcc.5b06923

corresponding to TiO_2 anatase was obtained (ICDD file no. 21-1272) with no perceivable traces of the rutile polymorph. Actually, to the eye of XRD, the increase in temperature merely returns a slim narrowing of the anatase peaks, indicating a slightly enhanced crystallinity in the particles of the new experiment (consistent with the higher temperature). No shifting of the anatase peaks is observed with respect to the anatase crystalline single-phase pattern, which indicates that crystal parameters do not change.

Further structural characterization was conducted by high resolution TEM. Images in Figure 3 reveal the presence of well-

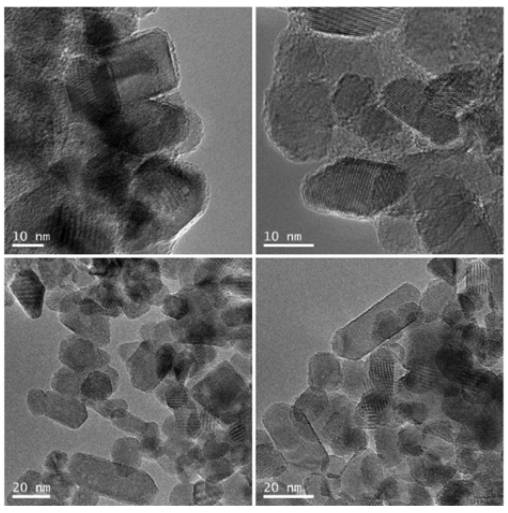

Figure 3. TEM micrographs of the anatase nanoparticles TiO_2-TFAA-Latt with different orientations.

faceted nanocrystals (15−20 nm) with broadly truncated rhombic shapes, again showing no big difference with the particles obtained at 200 °C. Interestingly, the rhombic shapes are consistent with Wulf type anatase nanoparticles exhibiting {101} and {001} facets.

Figure 4 depicts the results of the FTIR analyses performed on both, previous and present, experiments. At first glance the two spectra show the same shape of the baseline and the same characteristic bands, so in general terms we may presume a similar picture to that already discerned for the sample treated at 200 °C: bonded through the oxygen atoms of the carboxylic group, the TFAA molecules reside chemisorbed on the surface

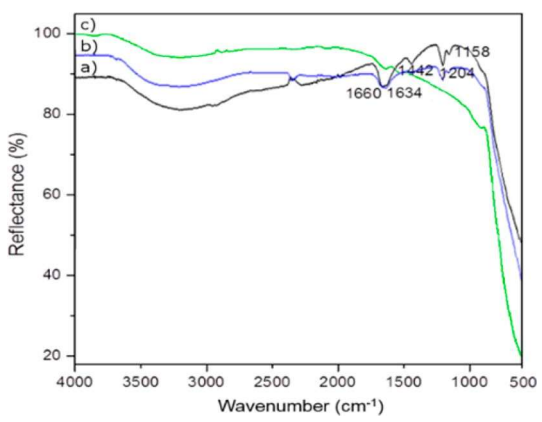

Figure 4. FTIR spectra of the (a) TiO_2-TFAA-Surf, (b) TiO_2-TFAA-Latt, and (c) Degussa P25 TiO_2 commercial catalyst.

of the TiO_2 crystals mainly in a bidentate mode.[29] But looking thoroughly to the intensity of the recorded IR bands, there is now one sizable difference between both samples, which is particularly significant for those bands assigned to TFFA: the C□O stretching vibrations at 1634 and 1442 cm^{-1} and the C−F stretching vibrations at 1204 and 1158 cm^{-1} exhibit a lower intensity when the sample is treated at 235 °C. Such diminution basically indicates a lower amount of TFAA adsorbed at the surface of the TiO_2 particles which, in turn, could obey to a larger decomposition of the TFFA molecule with the higher temperature.

High resolution XPS analyses in Figure 5 correspond to the F 1s core level photoemission of both samples and as depicted

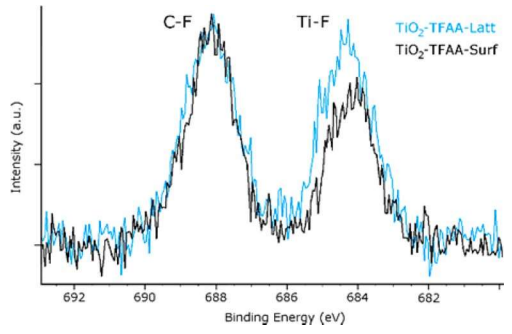

Figure 5. High resolution XPS spectrum corresponding to F 1s region for the TiO_2-TFAA-Surf and TiO_2-TFAA-Latt samples.

two main components are easily discriminated: the C−F component at ∼688 eV, which can be mostly related to $-CF_3$ groups of the TFAA molecule adsorbed on the surface of the TiO_2 particles, and the Ti−F component at ∼684 eV ascribed to an F−Ti−O chemical environment,[23,38−40] being indicative of the presence of Ti−F species at the crystal surface. Visibly the proportion between these two components has decreased for the blue precipitate obtained at 235 °C, indicating either a lower amount of $-CF_3$ groups or a higher quantity of free adsorbed F^-; whatever predominates, both cases again point toward a larger degradation of TFAA with the intended increment in the reaction temperature.

In order to quantify the real amount of F in the prepared samples, we analyzed the amount of fluorine what remains in the mother liquor after the reaction, being not significant. Therefore, it is expected that practically all the added fluorine is incorporated in the solid as F in the surface and within the TiO_2 particles and also, in a small amount, as trifluoroacetic acid adsorbed on the crystal surface.

Electron Magnetic Resonance and Optical Characterization. As indicated above the occurrence of the blue color in the powder obtained at 235 °C may be ascribed to the presence of Ti^{3+} centers in the anatase lattice. To further confirm this point we have conducted EPR measurements. X-band CW-EPR spectra of the sample were recorded at room temperature and at 77 K in air and under vacuum. The spectra are reported in Figure 6 (a-c).

At room temperature the baseline of the EPR spectrum is flat (Figure 6a) and no trace of paramagnetic species is observed in such conditions. Lowering the temperature to 77 K an intense EPR signal shows up at g values lower than the free electron value (Figure 6b). The structure of the spectrum (which is clearly appreciable in spite of the wide line width) is axial with $g_\perp = 1.992$, $g_\parallel = 1.962$. These features of the g tensor are typical

DOI: 10.1021/acs.jpcc.5b06923

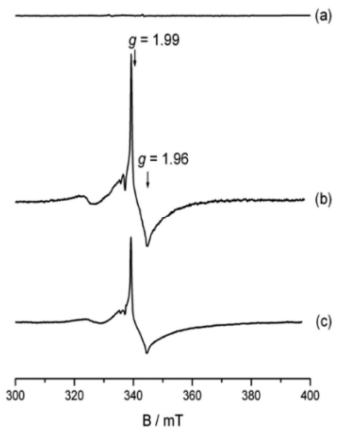

Figure 6. X band CW-EPR spectra of the as prepared TiO_2-TFAA-Latt sample recorded in air at room temperature (a) and at 77 K (b). Line c reports the spectrum of the same material recorded at 77 K under vacuum.

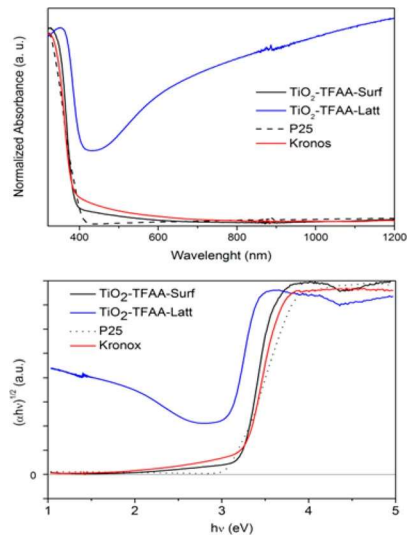

Figure 7. (a) DR UV−vis−NIR spectra and (b) Tauc plot from the UV−vis absorption spectra corresponding to the TiO_2-TFAA-Surf, TiO_2-TFAA-Latt and Degussa P25 and Kronos TiO_2 commercial catalysts.

of Ti^{3+} ions in octahedral-type symmetry. The spectrum does not change significantly upon outgassing the sample (Figure 6c). The observed g tensor values are the same found in other cases of modified anatase powders. In particular, in the case of previously reported EPR studies of fluorine doped TiO_2 samples the same axial spectrum was observed though with narrower line width due to the low concentration of Ti^{3+} centers.[41] The spectra reported in Figure 6 are thus amenable to the presence of Ti^{3+} centers in the solid. The absence of a spectral trace at room temperature could be due to charge detrapping at elevated temperature. However, this interpretation remains an hypothesis since most Ti^{3+} signal vanish at temperatures near room temperature because of their intrinsic relaxation time. The large line width observed for the spectra in Figure 6 is due to the relatively high concentration of such centers which causes dipolar broadening of the spectral line. This is confirmed comparing the spectra with those reported in the literature[41] and generated by annealing under vacuum at increasing temperature an F-doped TiO_2 sample. The starting spectrum observed for the as prepared material is, as mentioned before, the same spectrum here reported with $g_\perp = 1.992$ and $g_\parallel = 1.962$ but with narrow line width. Annealing under vacuum causes a progressive loss of oxygen, with the consequent formation of excess electrons in the solid which are stabilized as Ti^{3+} centers. The effect observed upon annealing[42] is therefore a progressive growth of the spectral intensity (the concentration of Ti^{3+} increases) paralleled by broadening of the signal (onset of dipolar interactions) which eventually assumes a shape strictly similar to that of the spectra in Figure 6. There is therefore no doubt that the EPR spectra here reported are due to Ti^{3+} centers typical of the bulk anatase lattice (see the Discussion). At variance with previously reported cases of F-doped TiO_2, here the starting material already contains a relevant concentration of reduced Ti centers as indicated also by its optical absorption in the visible region which is absent in the materials with low F concentration.

Finally Figure 7 depicts the UV−vis diffuse reflectance spectra for both, white and blue, powders. As a tangible difference an onset of visible and NIR absorption occurs in the blue sample which, obviously, is not observed for the white sample. The band gap value was estimated from the corresponding Tauc plot ($(\alpha h\nu)^{1/2}$ vs $h\nu$). As illustrated while the absorption edge of the white powder yields a band gap of 3.20 eV, the accepted value for TiO_2 anatase, the blue precipitate displays an exceptional lower bandgap of 3.01 eV.

4. DISCUSSION

FTIR and XPS analyses both suggest that the increase in the synthesis temperature of the solvothermal reaction neatly provokes an increased degradation of the starting TFAA. Eventually this leads to a fine-tuning of the anatase electronic structure which is evidenced by the stable blue color of the as-obtained powders and, behind this, by the formation of a large number of EPR-visible Ti^{3+} centers. Indeed, the following two major mechanisms can account for the formation of the bulk Ti^{3+} ions in these samples: On the one hand the higher degradation of TFAA first produces a higher release of free fluoride ions to the medium, which substantially increases the doping capacity of the reacting system. Fluorine substitutes oxygen in the lattice and Ti^{3+} centers are then formed via a mechanism of valence induction whereby the extra-electrons borne by fluorine is stabilized by Ti cations. The resulting composition of the solid can be written as $Ti^{4+}_{(1-x)}Ti^{3+}_xO^{2-}_{(2-x)}F^-_x$. Moreover, EPR measurements unambiguously indicate that those excess electrons are specifically localized (stabilized) by regular lattice Ti^{4+} cations of the oxide bulk: the axial signal with components at $g_\perp = 1.992$ and $g_\parallel = 1.962$ appears when titania is doped with elements bearing an extra-electron with respect to titanium and oxygen (this is the case also of pentavalent metallic elements such as niobium or antimony)[42] or when electrons are injected in mild conditions by contact with reactive elements such as atomic hydrogen or alkaline metals.[43] Since the signal here reported is typical of the unperturbed solid (signals obtained with bare anatase by other reduction methods have different features) it must be associated with the regular crystallographic site typical of the anatase bulk;[43,44] this assignment is also corroborated by theoretical investigations.[45]

Additionally, the higher degradation of the TFAA organic molecules also produces a highly reducing atmosphere within the material during the solvothermal process. Titanium dioxide is a reducible compound whose composition greatly depends

DOI: 10.1021/acs.jpcc.5b06923

on the oxygen pressure. Therefore, a reducing atmosphere will tangibly encourage the formation of Ti^{3+} reduced species and the fact is that when HF is used as the fluorine source no such atmosphere is created (no organic matter being degraded) and, consequently, the number of Ti^{3+} centers is clearly lower as evidenced by EPR analyses.[42]

In other words, all EPR results previously reported concerning F-doped titania show the same signals here reported but with much narrower line width.[41,42] Since the line intensity and the large line width observed in the present case correspond to a higher number of reduced Ti^{3+} centers exhibiting mutual dipolar interaction, it can easily be concluded that the synthetic method here illustrated is much more efficient than those reported before in introducing fluorine ions into the lattice of anatase.

Obviously, this extensive fluorine doping of the anatase lattice and the subsequent formation of a large number of Ti^{3+} centers will have an influence in the optoelectronic behavior of the doped material. In this sense, the origin of the lower energy of the band gap is likely to be related to the presence, localization, and amount of these Ti^{3+} centers: As it has been demonstrated the energy levels corresponding to the Ti^{3+}-reduced states are extremely shallow;[42] the excess electrons tend to be delocalized over several of these Ti centers and consequently the Fermi level lies at the boundary or even in the lower region of the conduction band. When the concentration of Ti^{3+} states is greatly increased, as in our case, a sort of sub-band is formed close to the bottom of the conduction band, eventually resulting in a small but clear red shift of the optical band gap transition, i.e., in a decrease of the band gap (almost 0.2 eV from that of pristine anatase). On the other hand, the broad absorption peak (Figure 7), having a maximum in the IR region and tailing into the visible one (which is the reason for the blue color assumed by the F doped samples) indeed indicates the presence of free carriers inside the solid.[46,47] This free carriers are related to the presence of Ti^{3+} and lattice fluorine ions within the anatase nanoparticles.

The experimental and theoretical data obtained indicates that we have an ordered atomic structure of the material, leading to a decrease of the band gap in 0.2 eV. These results differs from those reported by Corradini et al.[48] who concludes that highly fluorinated anatase lattice with O vacancies is strongly disordered and leads to a strong decrease (by 0.8 eV) of the band gap compared to conventional anatase. This difference can be ascribed to in our case fluorine substitutes oxygen in the lattice and Ti^{3+} centers are then formed via a mechanism of valence induction whereby the extra-electrons borne by fluorine is stabilized by Ti cations. The resulting composition of the solid can be written as $Ti^{4+}_{(1-x)}Ti^{3+}_{x}O^{2-}_{(2-x)}F^{-}_{x}$. While, in the material reported by Corradini et al.[48] the presence of Ti^{3+} is not detected. The absence or low concentration of Ti^{3+} probably can stabilized the extra-electrons borne by fluorine leading to a different material whose general chemical formula is $Ti_{1-x}\square_x X_{4x}O_{2-4x}$ ($X^- = F^-$ or OH^-) with a strongly disordered atomic structure.

Photocatalytic Performance. The highly faceted morphology of the synthesized F-doped anatase nanoparticles together with the improved doping capability of the system eventually allow an enhanced UV photocatalytic performance. Figure 8 shows such photoactivity upon the degradation of methyl orange, evidencing how the change from a surface doped material (TiO_2-TFAA-Surf) to a lattice doped one (TiO_2-TFAA-Latt) undeniably provokes a faster response;

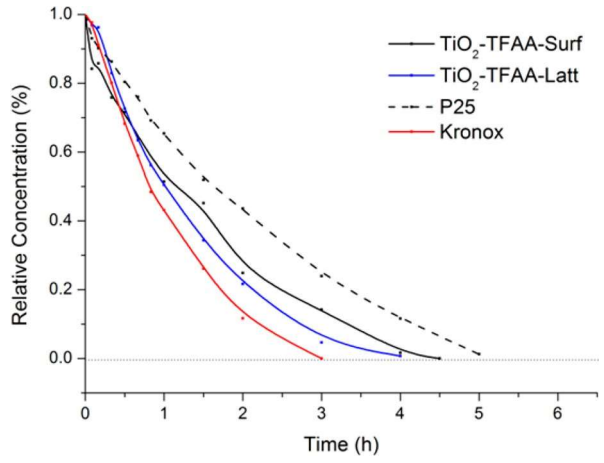

Figure 8. Evolution with the reaction time of methyl orange for the TiO_2-TFAA-Latt, TiO_2-TFAA-Surf, P25, and Kronos photocatalysts under UV light. Results are normalized on the weight of the solids.

moreover, it is clearly faster than that of Degussa P25 TiO_2 commercial catalyst, and gets closer to that of Kronos, another commercial catalyst based on TiO_2 but doped with Carbon instead of Fluorine.

But as described, the higher incorporation of fluorine ions into the anatase lattice also provokes the observed reduction in the bandgap of TiO_2, which now falls in the vicinity of the visible region: 3.01 eV. According to this value, an improved visible-light response of the produced nanoparticles would be expected. However, we have carried out some additional photocatalytic experiments which, unfortunately, indicated that a substantial improvement in the solar energy conversion is still hindered. This may indicate that a band gap reduction is not enough to guarantee a photocatalytic activity in the visible.

More specifically Figure 9 compares the activity of our blue powder with the other three photocatalysts on the degradation

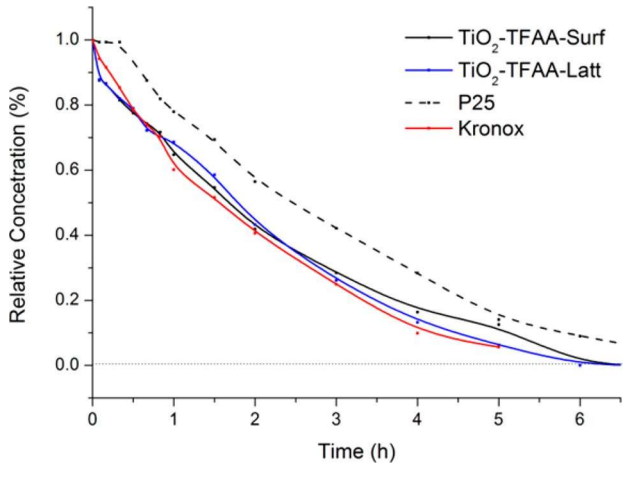

Figure 9. Evolution with the reaction time of methyl orange for the TiO_2-TFAA-Latt, TiO_2-TFAA-Surf, P25, and Kronos photocatalysts under visible light. Results are normalized on the weight of the solids.

of methyl orange under visible light. The fact is that these three other powders, P25, Kronos and our previous TiO_2-TFAA-Surf they all have a bandgap around 3.2 eV but as observed, the narrower bandgap of the blue titania is not clearly leading to a better visible light harvesting. Actually this unfavorable behavior has been already observed and attributed to an undesirably fast

DOI: 10.1021/acs.jpcc.5b06923

charge recombination occurring at the dopant centers, impeding the charge transfer from bulk to the surface and hence restraining the photocatalytic performance.[1,49] A clear conclusion from the present findings is that the existence of a narrower band gap does not necessarily lead to a better photocatalytic performance under visible light, a fact which has also been highlighted in the literature.

5. CONCLUSIONS

Highly crystalline fluorine-doped anatase nanoparticles have been prepared applying a modified one-step semi solvothermal methodology which also allows a more effective doping process, changing from a surface doped material to a lattice doping scenario. This is evidenced by the great number of Ti^{3+} centers occurring in the material, which mainly form to stabilize the extra electrons produced when fluorine substitutes oxygen in the TiO_2 lattice. As a first consequence the obtained blue powders exhibit an improved UV photocatalytic response. But more interestingly, upon lattice doping, the electronic structure of anatase TiO_2 is also fine-tuned and eventually its bandgap is narrowed making it closer to the visible region. Initially this remarkable result would open the doors for an increased solar energy conversion; unfortunately, a fast charge recombination is likely to happen at these dopant centers which still hinders the visible light harvesting, so new experiments must be envisaged to prevent or at least reduce that charge recombination process while preserving the reduced bandgap.

AUTHOR INFORMATION

Corresponding Author

*(D.G.C.) E-mail: dgcalatayud@icv.csic.es. Telephone: 0034 917355840.

Present Address

▽Department of Chemistry, University of Bath, Claverton Road, BA2 7AY, Bath, U.K.

Author Contributions

The manuscript was written through contributions of all authors. All authors have given approval to the final version of the manuscript.

Notes

The authors declare no competing financial interest.

ACKNOWLEDGMENTS

This work was supported by the Spanish Ministry of Economy and Competitiveness (MINECO) through the projects IPT-2011-1113-310000 (NANOBAC), MAT2013-40722-R (SCOBA), MAT2013-47878-C2-1-R and CTQ2012-30751 and by the Comunidad de Madrid through the project MULTIMAT-CHALLENGE P2013/MIT-2862. T.J. also acknowledges the European Science Foundation (ESF).

ABBREVIATIONS

TFAA, trifluoroacetic acid; TiO_2-TFAA-Latt, lattice-doped TiO_2 nanoparticles; TiO_2-TFAA-Surf, surface-doped TiO_2 nanoparticles; P25, Degussa P25 TiO_2 commercial catalyst; TEM, transmission electron microscopy; FTIR, Fourier transform infrared spectroscopy; XPS, X-ray photoelectron spectroscopy; EPR, electron magnetic resonance; NIR, near infrared; UV−vis, ultraviolet−visible; DRS UV−vis−NIR, ultraviolet−visible-near-infrared diffuse reflectance spectroscopy

REFERENCES

(1) Xu, H.; Ouyang, S.; Liu, L.; Reunchan, P.; Umezawa, N.; Ye, J. Recent Advances in TiO_2-based Photocatalysis. *J. Mater. Chem. A* 2014, *2*, 12642−12661.

(2) Asahi, R.; Morikawa, T.; Ohwaki, T.; Aoki, K.; Taga, Y. Visible-light Photocatalysis in Nitrogen-doped Titanium Oxides. *Science* 2001, *293*, 269−271.

(3) Khan, S. U. M.; Al-Shahry, M.; Ingler, W. B. Efficient Photochemical Water Splitting by a Chemically Modified n-TiO_2. *Science* 2002, *297*, 2243−2245.

(4) Chen, X.; Liu, L.; Yu, P. Y.; Mao, S. S. Increasing Solar Absorption for Photocatalysis with Black Hydrogenated Titanium Dioxide Nanocrystals. *Science* 2011, *331*, 746−750.

(5) Setvin, M.; Aschauer, U.; Scheiber, P.; Li, Y. F.; Hou, W.; Schmid, M.; Selloni, A.; Diebold, U. Reaction of O_2 with Subsurface Oxygen Vacancies on TiO_2 Anatase (101). *Science* 2013, *341*, 988−991.

(6) Chen, J.; Li, G.; Zhang, H.; Liu, P.; Zhao, H.; An, T. Anatase TiO_2 Mesocrystals with Exposed (001) Surface for Enhanced Photocatalytic Decomposition Capability Toward Gaseous Styrene. *Catal. Today* 2014, *224* (s), 216−224.

(7) Xu, Q.; Yu, J.; Zhang, J.; Zhang, J.; Liu, G. Cubic Anatase TiO_2 Nanocrystals with Enhanced Photocatalytic CO_2 Reduction Activity. *Chem. Commun.* 2015, *51*, 7950−7953.

(8) Tong, H.; Ouyang, S.; Bi, Y.; Umezawa, N.; Oshikiri, M.; Ye, J. Nano-photocatalytic Materials: Possibilities and Challenges. *Adv. Mater.* 2012, *24*, 229−251.

(9) Pan, X.; Yang, M. Q.; Fu, X.; Zhang, N.; Xu, Y. J. Defective TiO_2 with Oxygen Vacancies: Synthesis, Properties and Photocatalytic Applications. *Nanoscale* 2013, *5*, 3601−3614.

(10) Wang, Y.; Wang, Q.; Zhan, X.; Wang, F.; Safdar, M.; He, J. Visible Light Driven Type II Heterostructures and Their Enhanced Photocatalysis Properties: A Review. *Nanoscale* 2013, *5*, 8326−8339.

(11) Yang, H. G.; Sun, C. H.; Qiao, S. Z.; Zou, J.; Liu, G.; Smith, S. C.; Cheng, H. M.; Lu, G. Q. Anatase TiO_2 Single Crystals With a Large Percentage of Reactive Facets. *Nature* 2008, *453*, 638−641.

(12) Liu, S.; Yu, J.; Jaroniec, M. Anatase TiO_2 with Dominant High-energy {001} Facets: Synthesis, Properties, and Applications. *Chem. Mater.* 2011, *23*, 4085−4093.

(13) Wen, C. Z.; Jiang, H. B.; Qiao, S. Z.; Yang, H. G.; Lu, G. Q. Synthesis of High-reactive Facets Dominated Anatase TiO_2. *J. Mater. Chem.* 2011, *21*, 7052−7061.

(14) Ye, L.; Mao, J.; Liu, J.; Jiang, Z.; Peng, T.; Zan, L. Synthesis of Anatase TiO_2 Nanocrystals with {101}, {001} or {010} Single Facets of 90% Level Exposure and Liquid-phase Photocatalytic Reduction and Oxidation Activity Orders. *J. Mater. Chem. A* 2013, *1*, 10532−10537.

(15) Pan, J.; Liu, G.; Lu, G. Q.; Cheng, H. M. On the True Photoreactivity Order of {001}, {010}, and {101} Facets of Anatase TiO_2 Crystals. *Angew. Chem., Int. Ed.* 2011, *50*, 2133−2137.

(16) Selcuk, S.; Selloni, A. Surface Structure and Reactivity of Anatase TiO_2 Crystals with Dominant {001} Facets. *J. Phys. Chem. C* 2013, *117*, 6358−6362.

(17) Liu, G.; Yu, J.; Lu, G. Q.; Cheng, H. M. Crystal Facet Engineering of Semiconductor Photocatalysts: Motivations, Advances and Unique Properties. *Chem. Commun.* 2011, *47*, 6763−6783.

(18) Yu, J.; Low, J.; Xiao, W.; Zhou, P.; Jaroniec, M. Enhanced Photocatalytic CO_2-Reduction Activity of Anatase TiO_2 by Coexposed {001} and {101} Facets. *J. Am. Chem. Soc.* 2014, *136* (25), 8839−8842.

(19) Hu, X. Y. Synthesis of Octagonal Microdisks Assembled From Anatase TiO_2 Nanosheets With Exposed {001} Facets. *Ceram. Int.* 2014, *40* (9), 15033−15043.

(20) Maurino, V.; Minero, C.; Mariella, G.; Pelizzetti, E. Sustained Production of H_2O_2 on Irradiated TiO_2-Fluoride Systems. *Chem. Commun.* 2005, 2627−2629.

(21) Lv, K.; Xu, Y. Effects of Polyoxometalate and Fluoride on Adsorption and Photocatalytic Degradation of Organic Dye X3B on TiO_2: The Difference in the Production of Reactive Species. *J. Phys. Chem. B* 2006, *110*, 6204−6212.

DOI: 10.1021/acs.jpcc.5b06923

(22) Xu, Y.; Lv, K.; Xiong, Z.; Leng, W.; Du, W.; Liu, D.; Xue, X. Rate Enhancement and Rate Inhibition of Phenol Degradation Over Irradiated Anatase and Rutile TiO_2 on the Addition of NaF: New Insight Into the Mechanism. *J. Phys. Chem. C* 2007, *111*, 19024−19032.
(23) Meng, X.; Qi, L.; Xiao, Z.; Gong, S.; Wei, Q.; Liu, Y.; Yang, M.; Wang, F. Facile Synthesis of Direct Sunlight-driven Anatase TiO_2 Nanoparticles by In Situ Modification with Trifluoroacetic Acid. *J. Nanopart. Res.* 2012, *14*, 1176.
(24) Padmanabhan, S. C.; Pillai, S. C.; Colreavy, J.; Balakrishnan, S.; McCormack, D. E.; Perova, T. S.; Gun'ko, Y.; Hinder, S. J.; Kellys, J. M. A Simple Sol-gel Processing for the Development of High-temperature Stable Photoactive Anatase Titania. *Chem. Mater.* 2007, *19*, 4474−4481.
(25) Lv, K.; Cheng, B.; Yu, J.; Liu, G. Fluorine Ions-mediated Morphology Control of Anatase TiO_2 with Enhanced Photocatalytic Activity. *Phys. Chem. Chem. Phys.* 2012, *14*, 5349−5362.
(26) Yu, W.; Liu, X.; Pan, L.; Li, J.; Liu, J.; Zhang, J.; Li, P.; Chen, C.; Sun, Z. Enhanced Visible Light Photocatalytic Degradation of Methylene Blue by F-doped TiO_2. *Appl. Surf. Sci.* 2014, *319*, 107−112.
(27) Yu, J. C.; Yu, J. G.; Ho, W. K.; Jiang, Z. T.; Zhang, L. Z. Effects of F^- Doping on the Photocatalytic Activity and Microstructures of Nanocrystalline TiO_2 Powders. *Chem. Mater.* 2002, *14*, 3808−3816.
(28) Fang, W. Q.; Wang, X. L.; Zhang, H. M.; Jia, Y.; Huo, Z. Y.; Li, Z.; Zhao, H. J.; Yang, H. G.; Yao, X. D. Manipulating Solar Absorption and Electron Transport Properties of Rutile TiO_2 Photocatalysts Via Highly n-type F-doping. *J. Mater. Chem. A* 2014, *2*, 3513−3520.
(29) Calatayud, D. G.; Jardiel, T.; Peiteado, M.; Fernandez, C.; Rocio, M.; Dona, J. M.; Palomares, F. J.; Rubio, F.; Fernandez, D.; Caballero, A. C. Highly Photoactive Anatase Nanoparticles Obtained Using Trifluoroacetic Acid as an Electron Scavenger and Morphological Control Agent. *J. Mater. Chem. A* 2013, *1*, 14358−14367.
(30) Tosoni, S.; Lamiel-Garcia, O.; Fernandez-Hevia, D.; Doña, J. M.; Illas, F. Electronic Structure of F-doped Bulk Rutile, Anatase and Brookite Polymorphs of TiO_2. *J. Phys. Chem. C* 2012, *116*, 12738−12746.
(31) Tosoni, S.; Lamiel Garcia, O.; Fernandez Hevia, D.; Illas, F. Theoretical Study of Atomic Fluorine Diffusion through Bulk TiO_2 Polymorphs. *J. Phys. Chem. C* 2013, *117*, 5855−5860.
(32) Lamiel-Garcia, O.; Tosoni, S.; Illas, F. Relative Stability of F Covered TiO_2 Anatase (101) and (001) Surfaces From Periodic DFT Calculations and Ab Initio Atomistic Thermodynamics. *J. Phys. Chem. C* 2014, *118*, 13667−13673.
(33) Gago, R.; Redondo-Cubero, A.; Vinnichenko, M.; Lehmann, J.; Munnik, F.; Palomares, F. J. Spectroscopic Evidence of NO_x Formation and Band-gap Narrowing in N-doped TiO_2 Films Grown by Pulsed Magnetron Sputtering. *Mater. Chem. Phys.* 2012, *136*, 729−736.
(34) Diebold, U.; Li, M.; Dulub, O.; Hebenstreit, E. L. D.; Hebenstreit, W. The Relationship Between Bulk and Surface Properties of Rutile TiO_2 (110). *Surf. Rev. Lett.* 2000, *07* (5−6), 613−617.
(35) Carter, E.; Carley, A. F.; Murphy, D. M. Evidence for O_2^- Radical Stabilization at Surface Oxygen Vacancies on Polycrystalline TiO_2. *J. Phys. Chem. C* 2007, *111*, 10630−10638.
(36) Deskins, N. A.; Dupuis, M. Intrinsic Hole Migration Rates in TiO_2 From Density Functional Theory. *J. Phys. Chem. C* 2009, *113*, 346−358.
(37) Hopper, E. M.; Sauvage, F.; Chandiran, A. K.; Graïzel, M.; Poeppelmeier, K. R.; Mason, T. O. Electrical Properties of Nb^-, Ga^-, and Y^-Substituted Nanocrystalline Anatase TiO_2 Prepared by Hydrothermal Synthesis. *J. Am. Ceram. Soc.* 2012, *95*, 3192−3196.
(38) Yang, X. H.; Li, Z.; Sun, C.; Yang, H. G.; Li, C. Hydrothermal Stability of {001} Faceted Anatase TiO_2. *Chem. Mater.* 2011, *23*, 3486−3494.
(39) Ni, C.; Zhang, Z.; Wells, M.; Beebe, T. P., Jr.; Pirolli, L.; Mendez De Leo, L. P.; Teplyakov, A. V. Effect of Film Thickness and the Presence of Surface Fluorine on the Structure of a Thin Barrier Film Seposited From Tetrakis-(dimethylamino)-titanium Onto a Si(100)-2 × 1 Substrate. *Thin Solid Films* 2007, *515*, 3030−3039.
(40) Senna, M.; Sepelak, V.; Shi, J.; Bauer, B.; Feldhoff, A.; Laporte, V.; Becker, K. D. Introduction of Oxygen Vacancies and Fluorine Into TiO_2 Nanoparticles by Co-milling With PTFE. *J. Solid State Chem.* 2012, *187*, 51−57.
(41) Czoska, A.; Livraghi, S.; Chiesa, M.; Giamello, E.; Agnoli, S.; Granozzi, G.; Finazzi, E.; Di Valentin, C.; Pacchioni, G. The Nature of Defects in Fluorine-Doped TiO_2. *J. Phys. Chem. C* 2008, *112*, 8951−8956.
(42) Biedrzycki, J.; Livraghi, S.; Giamello, E.; Agnoli, S.; Granozzi, G. Fluorine and Niobium Doped TiO_2: Chemical and Spectroscopic Properties of Polycrystalline n-type Doped Anatase. *J. Phys. Chem. C* 2014, *118*, 8462−8473.
(43) Livraghi, S.; Chiesa, M.; Paganini, M. C.; Giamello, E. On the Nature of Reduced States in Titanium Dioxide As Monitored by Electron Paramagnetic Resonance. I: The Anatase Case. *J. Phys. Chem. C* 2011, *115*, 25413−25421.
(44) Chiesa, M.; Livraghi, S.; Paganini, M. C.; Giamello, E. Charge Trapping in TiO_2 Polymorphs as Seen by Electron Paramagnetic Resonance Spectroscopy. *Phys. Chem. Chem. Phys.* 2013, *15*, 9435−9447.
(45) Di Valentin, C.; Pacchioni, G.; Selloni, A. Reduced and n-Type Doped TiO_2: Nature of Ti^{3+} Species. *J. Phys. Chem. C* 2009, *113*, 20543−20552.
(46) De Trizio, L.; Buonsanti, R.; Schimpf, A. M.; Llordes, A.; Gamelin, D. R.; Simonutti, R.; Milliron, D. J. Nb-Doped Colloidal TiO_2 Nanocrystals with Tunable Infrared Absorption. *Chem. Mater.* 2013, *25*, 3383−3390.
(47) Khomenko, V. M.; Langer, K.; Rager, H.; Fett, A. Electronic Absorption by Ti^{3+} Ions and Electron Delocalization in Synthetic Blue Rutile. *Phys. Chem. Miner.* 1998, *25*, 338−346 (and references therein)..
(48) Corradini, D.; Dambournet, D.; Salanne, M. Tuning the Electronic Structure of Anatase Through Fluorination. *Sci. Rep.* 2015, *5*, 11553.
(49) Zhang, C.; Chen, S.; Mo, L. E.; Huang, Y.; Tian, H.; Hu, L.; Huo, Z.; Dai, S.; Kong, F.; Pan, X. Charge Recombination and Band-edge Shift in the Dye-sensitized Mg^{2+}-doped TiO_2 Solar Cells. *J. Phys. Chem. C* 2011, *115*, 16418−16424.

DOI: 10.1021/acs.jpcc.5b06923